Proc Indian Natn Sci Acad, **70, A** No.1, January 2004, pp.39–51

ATMOSPHERIC NEUTRINOS: PROBE BEYOND THE STANDARD MODEL

SHASHIKANT R DUGAD
Tata Institute of Fundamental Research, Colaba, Mumbai 400 005 (India)

(Received 16 February 2003; Accepted 30 June 2003)

Atmospheric neutrinos are produced through interactions of cosmic rays in the atmosphere. They were first detected in 1965 and have been studied extensively since then. The detection of atmospheric neutrinos requires large-area detectors located deep underground. Observations from several experiments involving different techniques have finally led to conclusive evidence for neutrino oscillations. We first discuss the neutrino physics relevant for atmospheric neutrino detection followed by our current knowledge on neutrino flux. We then review observations made by past and current experiments and their consequences for the Standard Model of particle physics. We conclude by summarising future prospects for atmospheric neutrino observations.

Key Words: Cosmic rays, Atmospheric Neutrinos, Standard Model, Super-Kamiokande, Neutrino Oscillations.

1 Introduction

Among known particles, neutrinos are the most weakly interacting particles and hence are quite difficult to detect experimentally. Neutrinos are produced in the atmosphere through cascade interactions of primary cosmic rays with air nuclei and subsequent decay of secondary particles. Primary cosmic rays at the TeV energy scale are mostly composed of protons and helium nuclei with a small fraction of heavier nuclei. On their interaction with air nuclei, they produce secondary particles such as pions, kaons etc. Atmospheric neutrinos are primarily produced through the decay of charged pions and subsequently muons as shown in the following decay chain,

$$\begin{aligned} \pi^{\pm} &\rightarrow \mu^{\pm} + \nu_{\mu}(\overline{\nu}_{\mu}) \\ \mu^{\pm} &\rightarrow e^{\pm} + \overline{\nu}_{\mu}(\nu_{\mu}) + \nu_{e}(\overline{\nu}_{e}) \, . \end{aligned}$$

As can be seen from the decay chain above, neutrinos in the atmosphere are predominantly produced in two flavours (ν_{μ}, ν_{e}). The flux of tau neutrinos (ν_{τ}) in the atmosphere is negligibly small as it requires copious production of mesons containing heavy quarks like charm and bottom. Since neutrinos are weakly interacting particles, large-area detectors with good target mass and tracking resolution are required to detect atmospheric neutrinos.

Since the flux of secondary particles in cosmic rays is extremely high at the surface as compared to the flux of neutrino-induced particles, neutrino detectors have to be located deep underground. Although shallow-depth locations can eliminate fluxes of most of the secondary particles, atmospheric muons still remain an irreducible background to the detection of events due to ν_{μ}-interaction. This background can be substantially reduced by placing the detector as deep as possible. For example, the flux of atmospheric muons beyond a zenith angle of 65° is quite small as compared to the flux of ν_{μ}-induced muons in the rock at the depth of 2 km[1]. In the early days, searches for atmospheric neutrinos were carried out using deep underground detectors with sufficiently good tracking ability. They were located at depths of 2–3 km. The detection of atmospheric ν_{μ}-induced muons was first reported in[2] 1965, just 3 years after the discovery[3] of muon neutrinos!

Atmospheric neutrinos are very powerful tools in the search for neutrino oscillations due to their wide energy range and the large variation in their propagation length before detection. They have been used successfully by experiments at Kamioka to provide clinching evidence for neutrino oscillation. In this article we first review neutrino physics pertaining to the study of atmospheric neutrinos and their role in the study of neutrino oscillation. We then discuss the estimation of fluxes of atmospheric neutrinos and

the techniques used to detect them. We conclude by summarising the exciting results from atmospheric neutrino experiments and the future directions in this field.

2 Neutrino Interactions

Atmospheric neutrinos interact with nucleons of nuclei or electrons of atoms via charged-current (CC) or neutral-current (NC) interactions. In the CC interaction, charged leptons are produced as a result of the interaction while the neutrino remains unchanged in the NC interaction. Here, we shall discuss only interactions with nucleons since the interaction with electrons is almost 1000 times smaller. Hence interactions with electrons do not contribute significantly to the observed data. The interaction of neutrinos depends on their energy and can be broadly classified as,

1a. CC Quasi-elastic scattering: $\nu + N \rightarrow l^{\pm} + N'$
1b. NC Elastic scattering: $\nu + N \rightarrow \nu + N$
2a. CC Single pion production: $\nu + N \rightarrow l^{\pm} + N' + \pi$
2b. NC Single pion production: $\nu + N \rightarrow \nu + N' + \pi$
3a. CC Multiple pion production:
$\nu + N \rightarrow l^{\pm} + N' + n\,\pi$
3b. NC Multiple pion production:
$\nu + N \rightarrow \nu + N' + n\,\pi$

The quasi-elastic CC interaction cross section dominates in the low energy region. At 1 GeV, almost 60% of the time, neutrinos interact with nucleons via this interaction. The single charged lepton that is produced carries almost all the neutrino energy. The cross section increases linearly at lower energy and then saturates[4,5] around 1 GeV.

In single pion production, the neutrino interacts with nucleons producing an unstable baryon. This baryon decays to produce a stable nucleon and a pion. The cross section for this process increases rapidly with energy and saturates around 2 GeV, and is comparable with quasi-elastic scattering[6,7].

Multiple pion production takes place when the invariant mass W of the νN system is more than 1.4 GeV/c^2. The number of pions produced in the interaction has a logarithmic dependence on W. Note that the multi pion production process is a dominant subset of the Deep Inelastic Scattering (DIS) process $\nu + N \rightarrow l^{\pm} + X$, where X may contain, in general, not only pions but also heavier mesons apart from a nucleon. Unlike quasi-elastic or single pion production, the cross section for multi pion production increases more or less linearly with the neutrino energy over a wide energy range[8,9]. This is also true for any DIS process involving heavier mesons.

In all cases, the NC interaction cross section is quite small as compared to the CC interaction of the same type. NC elastic scattering does not provide any observable experimental signature whereas NC interaction with pion production can be detected only if it takes place inside or in the close vicinity of the detector.

3 Atmospheric Neutrino Fluxes

In order to search for neutrino oscillations in the data, it is important to know as precisely as possible both the fluxes of neutrinos in the atmosphere and their interaction cross section. Inputs to the estimation of the flux are primarily, a) the energy spectrum of primary cosmic rays b) the energy spectrum of muons produced through decay of secondary particles such as pions and kaons c) modelling of the interaction of cosmic rays and secondary particles with the air nuclei d) modelling of geomagnetic effect on the flux of cosmic rays and e) modelling of the longitudinal development of extensive air showers produced by the cosmic rays.

Several groups have predicted the flux of neutrinos in the energy range of 1 GeV to 10^4 GeV[10]. The energy range of cosmic rays relevant for this is about 10 times higher than the neutrino energy range. The composition and the energy spectrum is better known from direct measurements upto 100 TeV, beyond which they are measured indirectly by sampling various components of air showers.

The energy spectrum of neutrinos is closely related to that of the muons as a function of altitude. Although the energy spectrum of muons is measured upto several TeV on Earth's surface, not enough data is available on its altitude dependence. Interaction of cosmic rays and secondary particles is modelled using accelerator-based data from hadron and heavy ion collision experiments. The data does not extend upto the required cosmic ray energy scale (10^{15} eV) and they need to be extrapolated.

The mean interaction distance of secondary particles such as pions and kaons increases with zenith angle thereby increasing the decay probability of these particles. This enhances the flux of muons and neutrinos in a slanted direction. This is referred as *the*

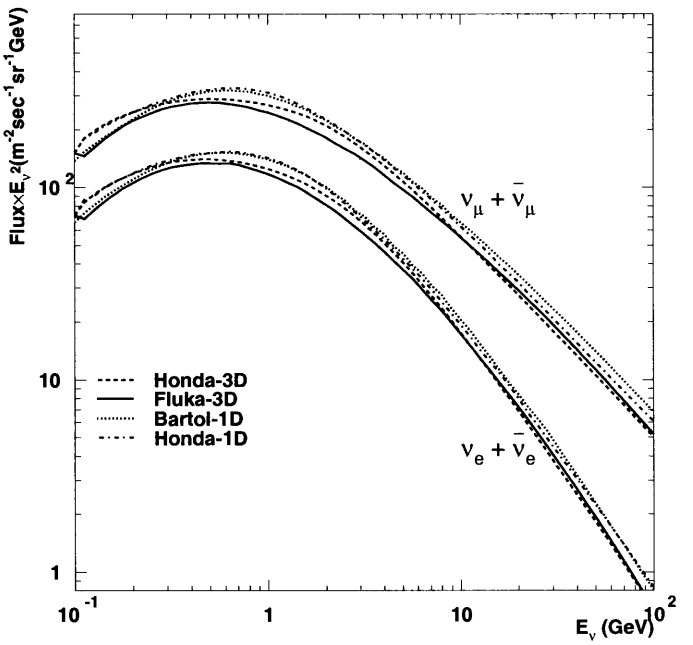

Fig. 1 Differential neutrino flux ($\times E_\nu^2$) at Kamioka location.

$\sec\theta$ *effect*; due to this, the fluxes of neutrinos increase gradually with zenith angle. As a result, the fluxes of neutrinos in the horizontal direction is estimated to be about 2 times higher than that in the vertical direction.

Uncertainties in each of the inputs mentioned above, due to limited availability of data, constrain the accurate estimation of the neutrino fluxes. The uncertainties in the neutrino flux are energy dependent and typically of the order of 20%. The flux of ν_e and ν_μ in the vertical direction is shown in Fig. 1.

Since the flux of cosmic rays is isotropic, the flux of neutrinos in the upward and downward direction is expected to be the same. However, due to geomagnetic field effects, the flux of low energy neutrinos ($E_\nu < 3$ GeV) gets modulated, resulting in an up-down asymmetry. This is shown in Fig. 2. As can be seen from this figure, the flux of neutrinos above 3 GeV is almost symmetric in the upward and the downward directions.

Once the fluxes of neutrinos and their interaction cross sections are known, the flux of ν_μ-induced muons (or electrons) can be computed. We consider two kinds of interactions: one where the neutrino interacts in the rock surrounding the (underground) detector, producing an energetic lepton that is detected in the detector, and another where the neutrino interaction and subsequent lepton detection occur within the detector.

The flux of muons produced by neutrino interaction in the surrounding rock can be evaluated by integrating the flux of ν_μ, weighted by the muon yield,

$$\mathrm{d}\mathscr{F}_\mu(E_\nu,\Theta) = \mathrm{d}\mathscr{F}_{\nu_\mu}(E_\nu,\Theta) \times Y_{[\nu_\mu\to\mu]}(E_\nu) \;, \ldots(1)$$

where $Y_{[\nu_\mu\to\mu]}$ is the muon yield *per* neutrino. The ν_μ-induced muon is assumed to maintain the original neutrino direction; an analogous formula holds for the $\bar{\nu}_\mu$-induced muon flux.

The muon yield increases with the energy of the neutrino and is calculated from the inclusive cross section for muon production $\mathrm{d}\sigma_{[\nu_\mu\to\mu]}$ and the number of target nucleons per cm^2. The yield of muons above the detector threshold energy, E_{min}, is given by

$$Y_{[\nu_\mu\to\mu]}(E_\nu) = \int_{E_{min}}^{E_\nu} \mathrm{d}E_\mu \frac{\mathrm{d}\sigma_{[\nu_\mu\to\mu]}}{\mathrm{d}E_\mu}(E_\nu,E_\mu) \times N_A\,[R(E_\mu) - R(E_{min})] \,. \quad \ldots(2)$$

Here N_A is the Avogadro number and $R(E_\mu)$ is the range of muons in the rock. The neutrino flux is known and can be obtained from ref.[10]. For the cross sections, the prescriptions of refs.[11–13] can be used for evaluating the energy dependence of various interaction processes described in Section 2.The range-energy dependence is illustrated in ref.[14]. The cross section and the range of muons increases

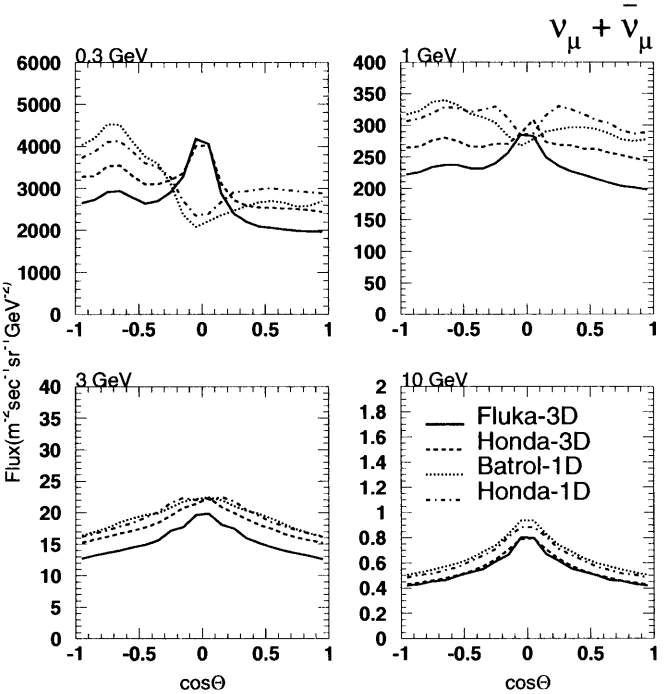

Fig. 2 Zenith angle distribution of neutrinos of different energies at Kamioka location[24].

more or less linearly with energy. Hence the energy spectrum of ν_μ-induced muons in the rock is much softer than that of the parent neutrinos.

When the $\nu-$induced muons (or electrons) are produced inside the detector's fiducial volume, the event rate is directly proportional to the fiducial mass (W) and can be evaluated using,

$$\text{Rate} = \int_\Omega \int_{E_\nu > E_{min}} dE_\nu \, d\Omega \, d\mathscr{F}_\nu(E_\nu, \theta) \, \sigma(E_\nu) \times W(tons) \, (10^6 \, N_A), \ldots (3)$$

where E_l^{min} is the energy threshold for a lepton of flavour l $(= e, \mu)$. Integration over neutrino energy has to be carried out above this threshold. For a given flavour the rate is the sum of contributions from ν_l and $\bar{\nu}_l$.

The flux of ν_μ and ν_e depends on the flux of muons produced through decay of pi/K in the atmosphere. Hence the uncertainties on the flux of each of them are highly correlated. Therefore, even if uncertainties on the absolute flux are high, the ratio of the ν-induced muon to electron events, for a given detector configuration, can be estimated more accurately. We have

$$R_{\text{theory}}(E) = \frac{N_\mu^{\text{exp}}(E)}{N_e^{\text{exp}}(E)}, \qquad \ldots (4)$$

where N_μ^{exp} and N_e^{exp} are the expected number of muons and electrons respectively. Here E is the energy of the charged lepton produced in the interaction. The ratio $R_{\text{theory}}(E)$ is predicted as a function of energy with an uncertainty better than 5%. It is to be noted that systematic effects due to detector response in obtaining this ratio experimentally are larger than theoretical errors. The decay probability of low energy muons in the atmosphere is higher as compared to that at high energy. Hence, for every ν_e there may be 2 ν_μ at low energy. Therefore the ratio R_{theory} is expected to be around 2 at low energy which will increase with lepton energy as shown in Fig. 3.

4 Atmospheric Neutrino Anomaly

The energy spectrum of low energy ν-induced muons and electrons has been measured experimentally using contained events. The detection techniques used for this measurement are described in Section 6. By understanding the detector response to electron and muon neutrinos, the ratio of the ν_μ-induced muon events to electron events has been measured in the low energy region by several experiments using contained event data-set and compared with predictions. This ratio is defined as,

$$R_{\text{obs}}(E) = \frac{N_\mu^{obs}(E)}{N_e^{obs}(E)}. \qquad \ldots (5)$$

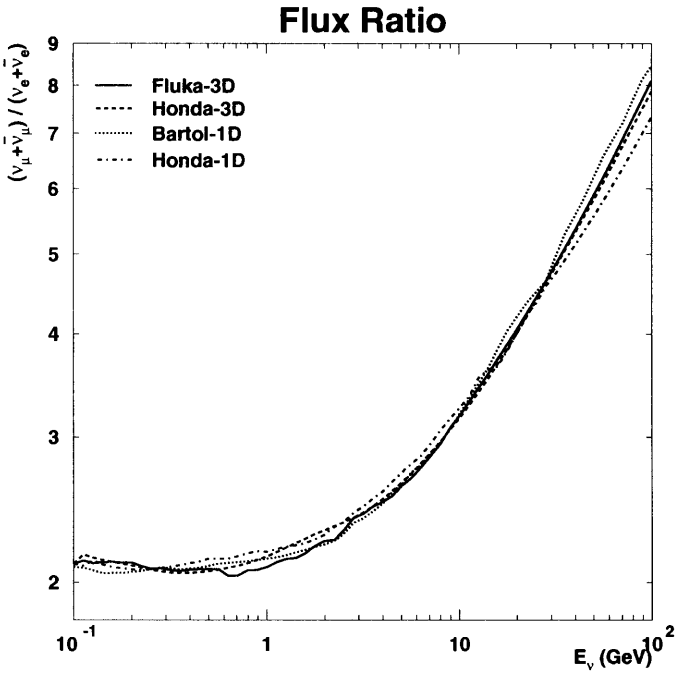

Fig. 3 Ratio of ν_μ to ν_e flux[24]

The ratio of ratio, RR_c,

$$RR_c(E) = \frac{R_{obs}(E)}{R_{theory}(E)} \qquad \ldots(6)$$

of contained events is expected to be unity but as can be seen from Table I, where results from various experiments are summarised, it deviates significantly from unity.

This observation was referred as *the atmospheric neutrino anomaly* and it is indicative of the existence of neutrino oscillation. However this measurement is sensitive to geomagnetic effect and detector response as a function of energy for both the flavours of neutrino; both of which are modelled through extensive Monte-Carlo (MC) simulation without enough experimental data. Based on these observations, the Super-Kamioka collaboration, in 1996, commissioned a very large volume detector with active volume of 50000 tons. This detector has not only confirmed the anomaly with high statistics but has also given evidence for neutrino oscillation. Results from this experiment are described in Section 7.

5 Neutrino Oscillations

In the standard model, neutrinos of all flavours are assumed to be massless. This would mean that neutrinos produced with certain flavour would remain in the same flavour at all times. However, if neutrinos are not massless then there is a possibility that neutrinos can change flavour as they propagate in space. This phenomenon is called as neutrino oscillation and originates from the mixing of flavour (weak) eigenstates. Neutrinos produced via weak interaction carry definite flavour (governed by the lepton number conservation). However, when it propagates in space, its mass eigenstate remains the same as that at production but its flavour content can change. The probability of flavour change depends on the mixing angle between flavours, the masses of the eigenstates, the energy of the neutrino and the distance travelled between point of production and detection. Observation of change in neutrino flavour is of great importance in particle physics since this will be the signature of breakdown of some of the vital assumptions made in the Standard Model. Within the 2-flavour vacuum oscillation model the flavour changing probability is given by,

$$P_{\alpha\to\beta}(E_\nu, L_\nu) = \sin^2(2\Theta_\nu) \times \sin^2\left(\frac{1.27\,\Delta m^2(eV^2)\,L_\nu(km)}{E_\nu(GeV)}\right), \qquad \ldots(7)$$

where α and β represent the flavour of neutrinos. As can be seen from the above expression, irrespective of neutrino masses the flavour and mass eigenstates are completely decoupled if the mixing angle Θ_ν is zero.

Table I
Summary of RR_c *measurements from earlier experiments*

Detector	Energy Range	Exposure (kton-year)	RR_c	Ref.
IMB	Sub-GeV	7.7	$0.54 \pm 0.05 \pm 0.01$	15
	Multi-GeV	2.1	$1.4^{+0.4}_{-0.3} \pm 0.3$	16
Kamiokande	Sub-GeV	7.7	$0.60^{+0.06}_{-0.05} \pm 0.05$	17
	Multi-GeV	6.0	$0.57^{+0.08}_{-0.07} \pm 0.07$	17
Soudan 2		3.9	$0.64 \pm 0.11 \pm 0.06$	18
Frejus		1.56	$1.00^{+0.15}_{-0.08}$	19
NUSEX		0.74	$0.96^{+0.32}_{-0.28}$	20

If the same is very small then it will be difficult to observe such a phenomenon experimentally. On the other hand if the mixing angle is sufficiently large, then the flavour changing probability will oscillate as a function of (L_ν/E_ν). Therefore, the probability of flavour change is often referred to as the oscillation probability. For $\Delta m^2 = 0.01 eV^2$ and neutrino energy of 1 GeV the oscillation probability is maximum at $L_\nu \sim 120$ km. If the distance travelled is very large as compared to the oscillation length, then the oscillation probability reaches the average value of $P_{\alpha \leftrightarrow \beta} \approx 0.5$ for a given energy spectrum of neutrino. In order to probe oscillation parameter space, therefore, we need an experimental setup which can span a wide range of L_ν/E_ν. Neutrinos coming from an accelerator do not have a wide energy range. Furthermore it is not feasible to move the detector over a wide range of distances *w.r.t.* to the neutrino source.

Atmospheric neutrinos offers all the desired features in a neutrino source for probing neutrino oscillations, that too free of cost! The distance travelled by the neutrino before its detection in the underground detector varies in the range of 10km $\sim$ 13000 km depending on the zenith angle (angle of incidence). The variation in the distance travelled as a function of the incident zenith angle of the neutrino is shown in Fig. 4. The energy of the neutrinos for events detected in the detector varies between 0.1 $\sim$ 1000 GeV. Hence the atmospheric neutrinos offer a wide dynamic range of 10^6 in L_ν/E_ν, thus making them a very powerful probe for studying the oscillation phenomenon.

As described in Section 4, the atmospheric neutrino anomaly suggests the possibility of oscillations but cannot confirm the same. There is yet another way to look for neutrino oscillations which is far more elegant and not very sensitive to either the geomagnetic effect or an accurate knowledge of the detector response. The distance travelled by neutrinos is significantly different for the upward and the downward directions. The distance travelled in the downward (upward) direction varies between 10-200 km (200 km - 13000 km) as shown in Fig. 4. If the Δm^2 for 2-flavour oscillation is in the range of 0.001 eV^2 to 0.01 eV^2, then for maximal mixing, the oscillation probability is quite small in the downward direction as compared to that in the upward direction. Hence we would expect an asymmetry in the ν-induced events in the detector for upward and downward direction for a given $|\cos\theta|$, where θ is the zenith angle. Therefore, if we can make sure that there is no asymmetry in the detector efficiency, one can look for oscillations by comparing the observed zenith angle distribution of events in the upward and downward directions. This is the cleanest channel to look for oscillation using atmospheric neutrinos and has been exploited successfully by the Super-Kamiokande detector.

6 Detection techniques

Ideally, the detector designed for detecting atmospheric neutrino interactions should be able to infer the flavour of the interacting neutrino, the energies and the directions of particles produced in the interaction, since each type of interaction provides a distinct event topology in the detector. For example, muon neutrino interacting inside the detector can give rise to partially or fully contained penetrating track. There are no prominent sources of background which can mimic this topology. The neutrino direction can be inferred by reconstructing the track. If the track is fully confined within the fiducial volume, then the energy of the muon can be inferred by the range of its track. This particular topology will correspond to quasi-elastic CC scattering of ν_μ. In case of CC ν_e-interaction, it would give rise to an electromagnetic cascade inside the detector. The neutrino interaction with multiple pion production (DIS) can give rise to several tracks as well as an electromagnetic cascade in the detector.

So far, we have mentioned event topologies gen-

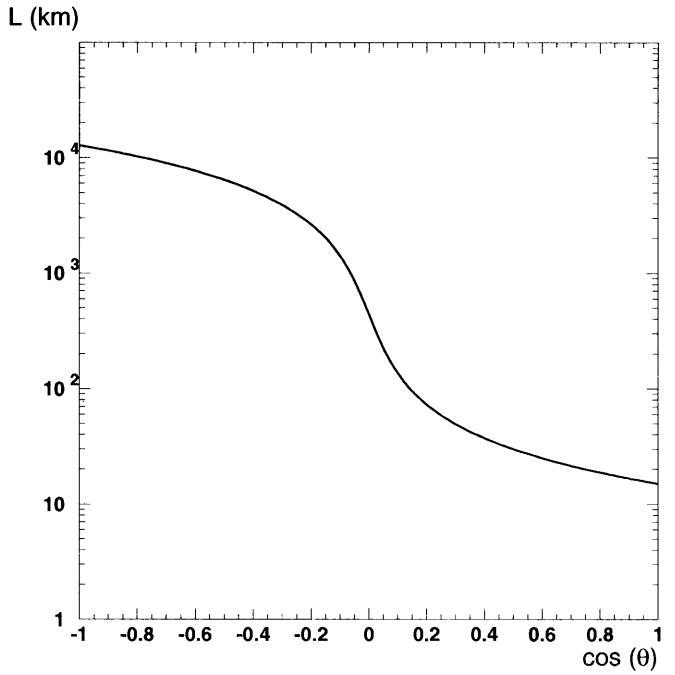

Fig. 4 Zenith angle dependence of distance travelled by neutrino in the Earth.

erated by interaction inside the detector. But muon neutrinos can also interact with the surrounding rock giving rise to a penetrating track in the detector. This particular topology has a huge background due to atmospheric muons coming from the surface. However, those detectors which can distinguish between upward and downward going muons can identify this topology without any ambiguity if the neutrino is propagating in the upward direction. In Fig. 5 we depict several topologies induced by the neutrino interactions. In order to study atmospheric neutrinos, the detector should be able to resolve different event topologies efficiently. For example, the gaseous fine grain calorimetric sampling detectors with good tracking resolution can be used to resolve most of the topologies. Several detectors, KGF, MACRO, SOUDAN[1,18,21] etc., in the early days employed this technique for studying atmospheric neutrinos. However these detectors have had serious limitations in distinguishing between the upward and downward directions of the track. To distinguish the up and down directions, one requires time of flight (TOF) measurement of particle along the track to the nanosecond accuracy. In the upgrade of MACRO detector, several well separated layers of scintillators were introduced to measure the TOF of the track.

In the early eighties large volume water Cerenkov detectors were commissioned for studying proton decay. These detectors contained large quantities of highly pure water surrounded by photo multiplier tubes (PMT). The passage of a charged particle (with sufficiently high energy) through water produces large number of Cerenkov photons in the form of a ring centered around its trajectory. The PMTs mounted on the surface of the detector are then used to detect these photons. The event topology is reconstructed using the timing and the signal size information from these tubes. Since there is no dead medium, these water Cerenkov detectors can measure energy deposited in the detector accurately. Furthermore they have excellent sensitivity to distinguish between the upward and downward directions for the through going muons as well as the contained events. However, none, of these detectors has a good sensitivity to study neutrino interaction with multiple pion production. Most of the important results are obtained using the data on quasi-elastic CC interaction events inside the detector and ν_μ-induced muon events in the surrounding rock.

7 Observations

Over the period of last 20 years, a large number of events due to neutrino interaction have been recorded by several detectors at different locations. These detectors have measured the flux of ν-induced muons and electrons using contained events and also the

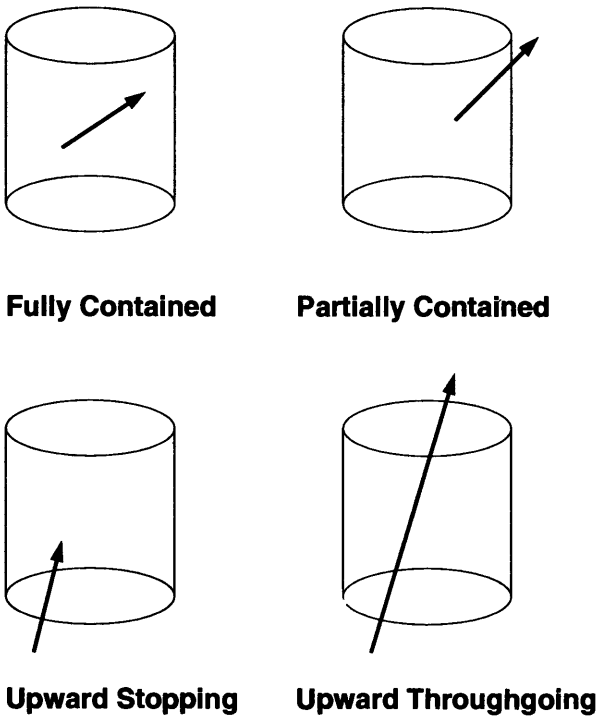

Fig. 5 Different event topologies induced by the neutrino interactions.

muons produced in the rock. Though the measured fluxes cannot be directly compared with the calculated fluxes, due to large uncertainty, as explained in Section 3, the ratio of the ν-induced muon to electron events has been measured and compared with predictions. The results from these experiments have been summarized in Table I. Based on this data, a large water Cerenkov detector (Super-Kamiokande[23]) was proposed in the late eighties. Since this detector has now given the first signal beyond the Standard Model, we shall present the observations from Super-K in detail followed by results from another more recent experiment (MACRO).

Super-Kamiokande (SK) Observations

This is the biggest detector in size and mass and has observed the largest collection of neutrino events. Observations made by other experiments which are relatively smaller in size, are more or less consistent with the results from this detector. Before presenting the data from this experiment, we describe the salient features of this experiment[23]. Super Kamiokande detector is located in the Kamioka mines of Gifu Prefecture, Japan. It has a mean overburden of 2700 mwe. It is a water Cerenkov detector, counting photons in the Cerenkov light generated by charged particles such as e, μ, π propagating in the water. It has a cylindrical shape (41.4 m height and 39.3 m in diameter) containing 50000 tons of highly purified water. The detector is segmented into two parts called the inner detector (ID) and the outer detector (OD). The OD is used as a veto detector. The dimension of the ID is 33.8 m (height) x 36.2 m (diameter). Cerenkov light produced in the water is detected by 7650 large area photo multiplier tubes (PMT) mounted on the side, top and bottom wall of the detector. The trajectory of a charged particle going through water is obtained by reconstructing Cerenkov ring using the timing and pulse height data from the PMTs the number of Cerenkov rings in an event corresponds to th number of particles generated in the interaction. The observed neutrino data in this detector can be broadly classified into two categories:

- *Partially or Fully contained (PC/FC) events:* These events are caused by ν_μ or ν_e interactions inside the detector. It is difficult to identify the flavour for ν-interaction with multiple pion production, therefore only events with single ring are used for the main analysis. The shape of the ring is used to identify the flavour of the incident neutrino. Passage of muon produces a sharp ring due to its energy loss mostly by ionization where as the Cerenkov ring produced by

Table II
Event statistics for various topologies in SK detector

Event Topology	Running Period	Live time (days)	No. of events
Contained (PC/FC)	May-96 to July-01	1489	12785
Upward through going Muons	April-96 to July-01	1678	1878
Upward Stopping muons	April-96 to July-01	1657	457

Table III
Event Summary of partially and fully contained events in SK detector with 91.6 k-ton years exposure

	Data	Monte Carlo	Data/MC	Ratio RR_c
Sub-GeV				
Fully Contained				
$1-$Ring	6447	6573.8	0.98	
$(e-$like)	3266	2665.2	1.23	
$(\mu-$like)	3181	3908.6	0.81	$0.664^{+0.017}_{-0.016} \pm 0.052$
$2-$Ring	1701	1658.2	1.03	
$\geq 3-$Rings	756	809.8	0.93	
Multi-GeV				
Fully Contained				
$1-$Ring	1436	1398.3	1.03	
$(e-$like)	772	603.2	1.28	
$(\mu-$like)	664	795.1	0.84	$0.653^{+0.036}_{-0.034} \pm 0.095$
$2-$Ring	583	620.8	0.94	
$\geq 3-$Rings	949	1012.9	0.94	
Partially Contained	913	1063.7	0.86	$0.663^{+0.030}_{-0.028} \pm 0.079$ (FC + PC 1-Ring Data)

the electron is much broader due to the production of electromagnetic cascade. There is practically no background for these type of events from atmospheric muons. Contained event data is divided into sub-GeV and multi-GeV range for the purpose of analysis.

- *Upward through going and stopping muons:* The ν_μ-induced muons in the surrounding rock propagate through the detector giving rise to sharp Cerenkov rings inside the detector. The rings may be accurately reconstructed if the path length inside the detector is sufficiently long. The upward and downward directions can be easily resolved from the timing information of pulses in PMT's. If a ring terminates within the detector, then it is identified as a stopping muon. There is overwhelming background for both these topologies (through going and stopping muons) due to the downward going atmospheric muons. However, there is no such background for upward going tracks and hence they can only come from ν_μ interactions in the surrounding rock.

The Super Kamioka detector started collecting data in 1996. Exposures for the data[24] presented here, are slightly different for different types of events and are indicated in Table II.

The through going and stopping muons are subjected to a minimum path length requirement of 7 meters corresponding to an energy loss of about 1.5 GeV in the detector. The contained events are further divided into two energy ranges and as per the number of rings associated with the event. In the case of single ring event, the flavour of the neutrino is identified using the shape of the ring. The data is divided into sub-GeV and multi-GeV. The sub-GeV range for electrons and muons are $0.1 < E^e_{vis} < 1.33$ GeV and $0.22 < E^\mu_{vis} < 1.33$ GeV respectively, where, E_{vis} is the visible energy deposited by the particle. The multi-GeV range for both the particles (e, μ) is $E_{vis} > 1.33$ GeV. Breakup of contained events is shown in Table III.The number of expected events estimated from Monte-Carlo (MC) estimates have large systematic uncertainties. However, as mentioned before, the ratio of ratios defined in eq. 6 should be consistent with unity within the statistical and systematic uncertainties. The overall systematic uncertainty from the expected ratio and detector response is about 10%. Statistical errors are about 2% which is quite small when compared to systematic errors. The ratio of ratios has been determined for both (sub-GeV and multi-GeV) the energy range and it deviates significantly from unity indicating depletion in the muon flux in both energy regions (Table III). They are consistent with observations made by earlier experiments shown in Table I.

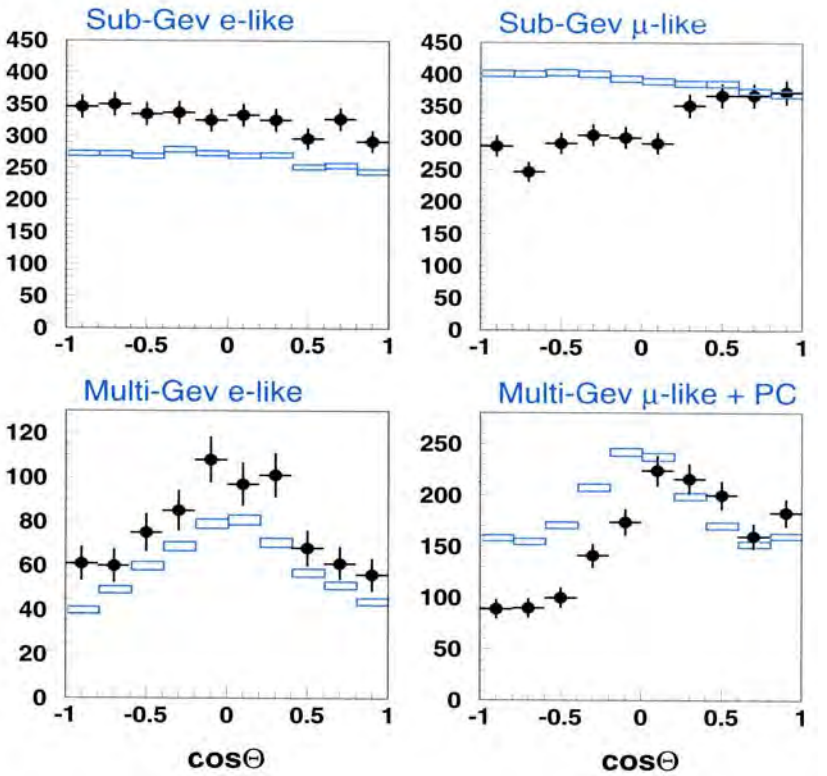

Fig. 6 Zenith angle distribution of observed no. of events in sub-GeV and multi-GeV range for electron and muon like events[24].

Due to the large data sample, the atmospheric neutrino anomaly can be investigated in more detail. The zenith angle distribution of the number of electron and muon-like events in different energy regions is shown in Fig. 6. Since the flux of neutrinos is roughly symmetric in upward and downward directions (ignoring geomagnetic effects in the low energy region), we expect observed number of events to be symmetric around $\cos\theta = 0$. As can be seen from Fig. 6, the observed shape of the distribution for electrons is indeed consistent with that expected, but for muons, a distinct asymmetry is observed around the horizon ($\cos\theta = 0$). This is referred to as the up-down asymmetry in muon flux and is independent of the many uncertainties that plague the neutrino fluxes, cross sections as well as the detector response. It is this observation that has given compelling evidence for the signal beyond Standard Model.

Another set of data in which neutrino interacts in the rock has also been looked at for possible depletion in the flux. The SK experiment has measured the flux of stopping and through going upward muons. Once again theoretical errors on each of these evens are quite large. However they get compensated to a large extent when the ratio of stopping to through going muons is estimated. The ratio of ratios for this type of events is obtained in a way similar to that of contained events (eq.6). It is measured to be $0.650 \pm 0.043 \pm 0.092$, again showing significant deviation from unity.

All the observations made by the SK experiment show that there is disappearance of muon neutrinos. No apparent inconsistency has been seen between various methods used in the data analyses as well as in the similar observations made by other experiments on atmospheric neutrinos. One of the most promising explanations for the disappearance is the oscillation of ν_μ to the ν_τ flavour. Many other models such as neutrino decay and oscillation into sterile flavours etc. have been ruled out to a good extent by these observations. The allowed region of oscillation parameters for $\nu_\mu \leftrightarrow \nu_\tau$ oscillation that explains all the features of the data is shown in Fig. 7. The best fit values in the physical region are $\Delta m^2 = 2.51 \times 10^{-3}$ eV^2 and $\sin(2\Theta_v) = 1$.

MACRO Observations

The MACRO experiment[22] conducted at the Gran Sasso laboratory is a large area detector with 14 layers of streamer tubes providing fine tracking and the scintillation counters measuring timing precisely. The

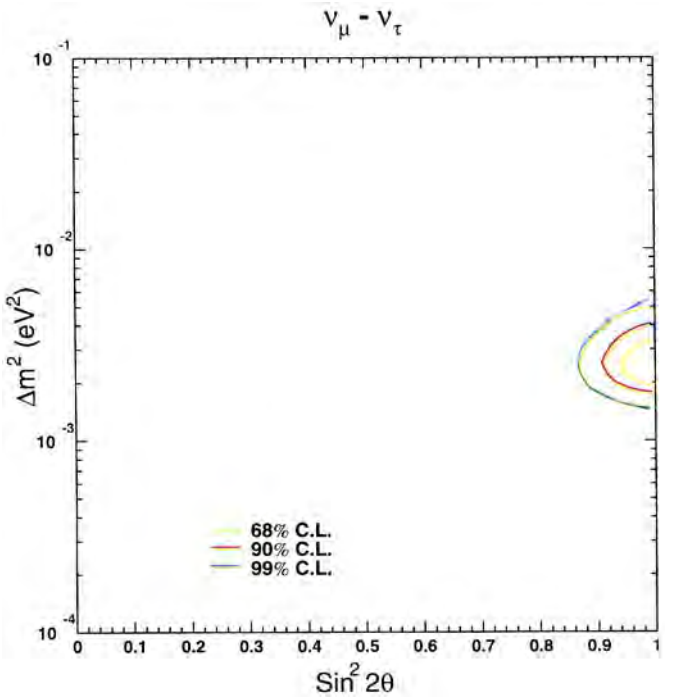

Fig. 7 Allowed region of oscillation parameter space under $\nu_\mu \leftrightarrow \nu_\tau$ oscillation[24]

experiment completed data taking in the year 2000 with a total live time of 5.52 years. The measured ratio of ratio[21] RR_c is $0.72 \pm 0.026 \pm 0.043 \pm 0.12$. The detector is also sensitive to the upward going muons with ν-interaction in the rock or inside the detector and the downward going muons with ν-interaction in the detector. The number of events observed for different types of events is summarized in Table IV. The

Table IV
Event statistics for various topologies in MACRO Detector

Event Topology	Signal Events	Background
Upward through going muons	809	54
Upward Stopping muons + Internally Downward going	262	10
Internally upgoing muons	154	7

shape of zenith angle distribution for upward going muons is shown to be sensitive to neutrino oscillations and other phenomena beyond Standard Model. The data[21] rejects null hypothesis with no oscillation and also disfavours oscillations into a sterile neutrino by $> 99\%$ CL. The data is consistent with 2-flavour (active) oscillation model, however, the range of allowed parameters obtained is wider than the corresponding range in SK results. It is consistent with the SK data.

8 Future Directions

The atmospheric neutrino anomaly observed by several earlier experiments has been confirmed by detailed observations at the Super Kamioka detector. Furthermore the results of SK and earlier detectors provide conclusive evidence for a signal beyond Standard Model. The most favourable explanation is the oscillation between ν_μ and ν_τ flavours. This explanation also provides consistency between solar and atmospheric neutrino observations. However, there are some other models which may explain various features in the atmospheric neutrino data. This is mainly because the *upward swing* in the up-down ratio is not yet clearly observed in the data and is crucial to establish neutrino oscillation hypothesis on a firm footing. The swing in the ratio is anticipated from the relatively high energy neutrinos and hence can be obtained only if we can probe the energy spectrum of muons induced by the higher energy neutrinos. In the SK detector muon energy can only be measured for the fully contained events. The fiducial volume drops rapidly as a function of the muon energy and hence the energy spectrum can only be measured in a small energy range for the muons. The up-down ratio is obtained using eq. 8 in different energy bins and is shown in Fig. 8.

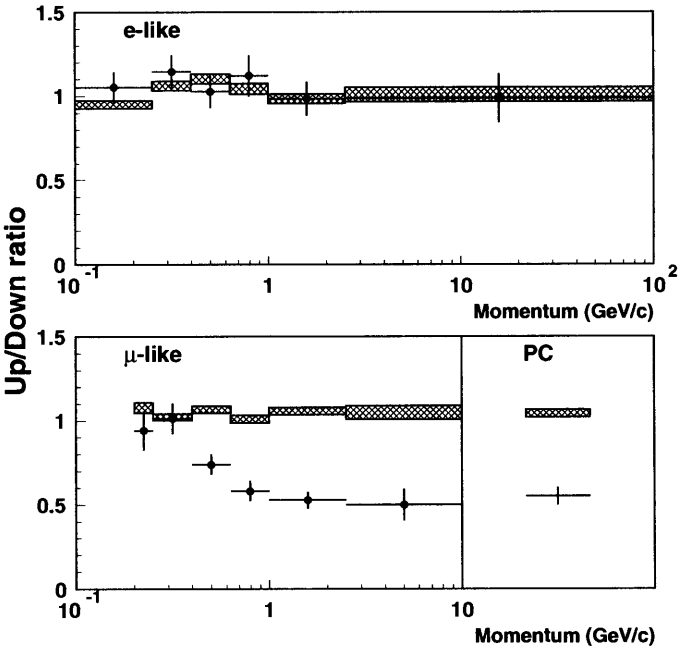

Fig. 8 Up/Down ratio for electron and muon like events[24].

$$R_{u/d}(E_\mu) = \frac{N_{up}(E_\mu/e, Cos\theta < -0.2)}{N_{down}(E_\mu/e, Cos\theta > 0.2)} \quad \ldots(8)$$

At low energies the ratio is close to unity. This can happen if the oscillation probability for downward and upward directions reaches the average asymptotic value, whereas, in the multi-GeV region, the ratio is close to 0.5. Probable explanation for this could be that the oscillation probability is very small in the downward direction whereas it has reached the asymptotic value in the upward direction. If we can sample sufficiently high energy neutrinos then we should be able to observe the turnaround (*upward swing*) of the ratio towards unity since the oscillation probability in both directions are very small. Among the existing observations, KGF atmospheric neutrino data combined with SK observations is expected to have the sensitivity to observe the upward swing in the oscillation probability[25]. Further the magnetic spectrograph type of detectors that are being planned[26,27] will allow such measurements with greater accuracy. These detectors can measure momentum of the muons for fully and partially contained events as well as the upward going muons and hence probing higher range of neutrino emerges to measure the spectrum. They would have the sensitivity to observe the full cycle of oscillation probabilities and also will have higher sensitivity to distinguish between the various models explaining SK observations. So far evidence for neutrino oscillations has only been seen as a disappearance of ν_μ to the ν_τ neutrino. In order to establish this beyond any doubts, it will be desirable to identify the events due to appearance of ν_τ interaction in the detector. It is extremely difficult to identify such an event. The ICARUS collaboration [28] is building a liquid argon calorimeter specially designed to identify events due to ν_τ-interaction in the detector.

9 Discussion

The Standard Model of particle physics has been firmly established over the last three decades. Experiments carried out with atmospheric neutrinos have given the first ever evidence challenging the Standard Model. Being the first signal, it has to be confirmed using different sources of neutrinos with more advanced experimental techniques. Current data strongly suggests the existence of neutrino oscillation. Future experiments are expected to confirm the source of this new signal and if it is indeed due to the oscillations they will measure the oscillation parameters more accurately. Observation of solar neutrinos also suggests the oscillation of electron neutrinos. All these results have formed the basis for changing our current understanding of the Standard Model. Probably this is just the beginning and the future appears to be exciting.

References

1 H R Adarkar *et al* in Proc 23th ICRC Calgary Vol **4** (1993) 487

2 Achar C V *et al Phys Lett* **18** (1965) 196; Achar C V *et al Phys Lett* **19** (1965) 78

3 G Danby *et al Phys Rev Lett* **9** (1962) 36

4 Framework for Quasi elastic neutrino interaction C H Llewellyn Smith *Phys Reports* **3** (1972) 261; P Lipari, M Lusignoli and F Sartogo *Phys Rev Lett* **74** (1995) 4384

5 Experimental data for Quasi elastic neutrino interaction A S Vovenkov *et al Yad Fiz* **30** (1979) 1014; S Barish *et al Phys Rev* D **16** (1977) 3103; S Bonetti *et al Nouvo Cimento* **38** (1977) 260; M Pohl *et al Nouvo Cimento* **26** (1979) 332; N Arimenise *et al Nucl Phys* B **152** (1979); S Belikov *et al Z Phys* **320** (1985) 625; C H Albright *et al Phys Rev* D **14** (1976) 1780; K Abe *et al Phys Rev Lett* **56** (186) 1107

6 Framework for neutrino interaction with single pion production D Rein and L M Sehgal *Ann of Phys* **133** (1981) 1780

7 Experimental data for neutrino interaction with single pion production G Radecky *et al Phys Rev* D **25** (1982) 116; T Kitagaki *et al Phys Rev* D **34** (1986) 2554; P Allen *et al Nucl Phys* B **264** (1986) 221; P Allen *et al Nucl Phys* B **176** (1980) 269; W Lerche *et al Phys Lett* **4** (1978) 510; J Bell *et al Phys Rev Lett* **15** (1978) 1008; D Allisis *et al Ann Phys* (1983) S J Barish *et al Phys Lett* B **91** (1980) 161; M Derrick *et al Phys Rev* D **23** (1981) 569

8 Framework for neutrino interaction with multiple pion production C H Albright and C Jarlskog *Nucl Phys* B **84** (1975) 467; M Glück, E Reya and A Vogt *Zeit Phys* C **67** (1995) 433; L Alvarez-Ruso, S K Singh and M J Vicente Vacas *Phys Rev* C **57** (1998) 2693

9 Experimental data for neutrino interaction with multiple pion production S J Barish *et al Phys Rev* D **17** (1978)1; P S Auchincloss *et al Z Phys* C **48** (1990) 411; P Berger *et al Z Phys* C **35** (1987) 443; S Campolillo *et al Phys Lett* B **84** (1979) 281; O Erriquez *et al Phys Lett* B **89** (1979) 309; J V Allaby *et al Z Phys* C **38** (1988) 403; N J Baker *et al Phys Rev* D **25** (1982) 617; C Baltay *et al Phys Rev Lett* **44** (1980) 916; D C Colley *et al Z Phys* C2, 187 (1979) 187; V B Anikeev *et al Z Phys* C **70** (1996) 39; A S Vovenko *et al Yad Fiz* **30** (1979) 187; D B MacFarlane *et al Z Phys* C **26** (1984) 1; D S Baranov *et al Phys Lett* B **81** (1979) 255

10 V Agrawal *et al Phys Rev* D **53** (1996) 1314; G Battistoni *et al Astroparticle Physics* **12** (2000) 315; M Honda *et al Phys Rev* D **64** (2001) 53011; Fluka model: http://pcfluka.mi.infn.it/

11 P Lipari, M Lusignoli and F Sartogo *Phys Rev Lett* **74** (1995) 4384

12 L Alvarez-Ruso, S K Singh and M J Vicente Vacas *Phys Rev* C **57** (1998) 2693

13 M Glück, E Reya and A Vogt *Zeit Phys* C **67** (1995) 433

14 P Lipari and T Stanev *Phys Rev* D **44** (1991) 3543

15 R Becker-Szendy *et al Phys Rev* D **46** (1992) 3720

16 R Clark *et al Phys Rev Lett* **79** (1997) 345

17 Y Fukuda *et al Phys Lett* B **335** (1994) 237

18 W W M Allison *et al Phys Lett* B **449** (1997) 137

19 K Daum *et al Z Phys* C **66** (1995) 417

20 M Aglietta *et al Europhysics Lett* **8** (1989) 611

21 MACRO Collaboration *Phys Lett* B **517** 59 (2001)59; MACRO Collaboration ICRC Proceedings (2001) 1069

22 MACRO Detector MACRO Collaboration M Ambrosio et al *Nucl Instr Methods Phys Res* A **486** (2002) 663–707

23 Super Kamiokande Detector description *To appear in NIM A* Accepted on 9-Jan-2003 See http://www-sk.icrr.u-tokyo.ac.jp/doc/sk/pub/index.html

24 Super Kamiokande Collaboration *Phys Rev Lett* **85** (2000) 3999; Super Kamiokande Collaboration *Phys Lett* B **467** (1999) 185; Atsuko Kibayashi *Ph.D. Thesis* (2002); Jun Kameda, *Ph.D. Thesis* (2002)

25 S R Dugad and F Vissani *Phys Lett* B **469** (1999) 171

26 INO Collaboration See website http://www.imsc.res.in/~ino/

27 MONOLITH Collaboration See website http://castore.mi.infn.it/~monolith/

28 ICARUS Collaboration *Nucl Inst Meth* A **498** (2002) 292